FRONTIERS OF PHYSICS

RESEARCH ARTICLE
Volume 18 / Issue 1 / 12501 / 2023

Nonreciprocal microwave transmission under the joint mechanism of phase modulation and magnon Kerr nonlinearity effect

Cui Kong[1], Jibing Liu[1,†], Hao Xiong[2,‡]

1 College of Physics and Electronic Science, Hubei Normal University, Huangshi 435002, China
2 School of Physics, Huazhong University of Science and Technology, Wuhan 430074, China
Corresponding authors. E-mail: †liujb@hbnu.edu.cn, ‡haoxiong1217@gmail.com
Received May 10, 2022; accepted August 18, 2022

ABSTRACT

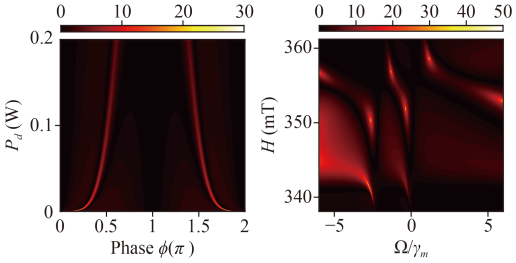

Nonreciprocal microwave devices, in which the transmission of waves is non-symmetric between two ports, are indispensable for the manipulation of information processing and communication. In this work, we show the nonreciprocal microwave transmission in a cavity magnonic system under the joint mechanism of phase modulation and magnon Kerr nonlinearity effect. In contrast to the schemes based on the standard phase modulation or magnon Kerr nonlinearity, we find that the joint mechanism enables the nonreciprocal transmission even at low power and makes us obtain a high nonreciprocal isolation ratio. Moreover, when two microwave modes are coupled to the magnon mode via a different coupling strength, the presented strong nonreciprocal response occurs, and it makes the nonreciprocal transmission manipulating by the magnetic field within a large adjustable range possible, which overcomes narrow operating bandwidths. This study may provide promising opportunities to realize nonreciprocal structures for wave transmission.

Keywords nonreciprocal microwave transmission, phase modulation, magnon Kerr nonlinearity effect

1 Introduction

Controlling matter–light interactions with cavities is of fundamental importance in not only the study of basic nonlinear dynamics in physics, but also advance modern technologies [1, 2]. Recently, a number of pioneering works have been accomplished in cavity magnon systems [3–8] due to the strong coupling between magnon excitations and microwave photons, which played crucial roles in quantum information processing [9–11]. Among them, the use of a small sphere of yttrium iron garnet (YIG) single crystals enables the strong [12–16] and even ultrastrong [17–19] magnon–photon couplings, thanks to its large spin density and low damping rate. Benefiting from the distinguishing advantages of strong coupling of cavity-magnon at room temperature, low loss magnetic materials, flexible controllability of the magnetic field, etc., these cavity magnonic systems have become a unique platform for exploring various intriguing phenomena, such as cavity magnon polariton (CMP) [20, 21], magnon gradient memory [22, 23], dissipative magnon–photon coupling [24–26], cavity spintronics [27, 28], exceptional points [29–31], and ground state cooling [32]. Moreover, due to the intrinsic magnetocrystalline anisotropy in the YIG, the magnon Kerr nonlinearity effect has been theoretically and experimentally demonstrated [33, 34]. Based on the magnon Kerr effect, the interesting phenomena, including entangled state [35], sub-Poissonian statistic [36], bistability of cavity magnon polaritons [21], magnon-induced high-order

https://doi.org/10.1007/s11467-022-1203-0

sideband [37, 38] and chaos [39], nonreciprocal transmission [40–42] have been novelly demonstrated.

Nonreciprocal transmission is a fundamental operation mechanism behind various nonreciprocal devices, such as light isolators, circulators and directional amplifiers, which plays crucially important roles in both basic research and applied science [43–45]. However, the nonreciprocity, which depends on the transmission characteristics related to the propagation direction under exchange of source and detector, is difficult to achieve due to the need to break the Lorentz reciprocity theorem. Until now, several common methods have been suggested for generating nonreciprocity, that is magneto-optic material responses [46, 47], the use of spatiotemporal modulation [48, 49] and optical nonlinear effects [50, 51]. Nevertheless, these physical schemes also have some drawbacks, such as unable to realize micro integration, harsh experimental conditions, or limited performance. Therefore, other possibilities are needed to achieve the nonreciprocal transmission by going beyond these methods. Very recently, by taking advantage of the unique cavity magnonic systems, many methods for generating nonreciprocal microwave transmission have been demonstrated. For example, there are the optical controllable method based four-wave mixing effect [52], by utilizing loss under multiple channels with interference [53, 54], making use of the selective coupling between the magnon mode and microwave modes with different chiralities [55, 56], and magnon Kerr nonlinearity [57].

Motivated by the previous proposals employing the phase modulation [58] and the nonlinearity effect [34], we theoretically propose a multimode cavity magnonic system to study the nonreciprocal microwave transmission under the joint mechanism of phase modulation and magnon Kerr nonlinearity effect. On the one hand, the magnon Kerr nonlinearity exists objectively in practice, which is usually regarded as complex and intractable in the standard interference-based schemes, but we find that the combined action of quantum interference induced by the phase difference and magnon Kerr nonlinearity effect not only enables nonreciprocal transmission to be observed at low power but also provides conditions for obtaining high isolation rates. On the other hand, taking advantage of adjustable magnetic field, when two microwave modes are coupled to the magnon mode via a different coupling strength, the effective operating bandwidth of the strong nonreciprocity can be broadened.

In this paper, we propose and analyze nonreciprocal microwave transmission based on a three-mode cavity magnonics system comprised of a superconducting ring resonator and a YIG sphere. We show that by harnessing a total phase difference-induced quantum interference among multiple channels, as well as the magnon Kerr nonlinearity originating from the nature of magnons, the variable nonreciprocity with wide bandwidth can be realized. In the scheme, we combine the phase modulation with the magnon Kerr nonlinearity effect to improve the nonreciprocal transmission, which has not been reported in cavity magnonics systems. Through dynamic modulation of the probe field or the external magnetic field, which has a great flexible controllability and is easy to operate in practice, high forward to backward incidence extinction ratios (>20 dB) [59] can be obtained, and to some extent, the unidirectional transmission of microwave waves may be achieved. Moreover, when two microwave modes are coupled to the magnon mode via a different coupling strength, the nonreciprocal response can be further enhanced, and meanwhile it can make the nonreciprocal transmission manipulating by the magnetic field within a large adjustable range possible, which overcomes narrow operating bandwidths. We expect this work to stimulate the exploration of physics and applications of isolators, circulators, directional amplifiers and so on.

The paper is organized as follows. In Section 2, we introduce a three-mode cavity magnonic system and demonstrate nonreciprocal microwave transmission under the joint mechanism of phase modulation and magnon Kerr nonlinearity effect. In Section 3, we show the nonreciprocal transmission adjusting by the probe field and the magnetic field under different conditions. In Section 4, a conclusion of the results is summarized.

2 Theoretical model and equations

The physical model we study is a waveguide-coupled superconducting ring resonator, with a YIG sphere, which is supported by a pedestal in the middle of the ring resonator, as shown in Fig. 1(a). There are two paths of propagating lights in the ring resonator, which includes pairs of degenerate clockwise (a_{cw}) and counterclockwise (a_{ccw}) microwave modes. In addition, a uniform external static magnetic field (H), which can be generated by a superconducting magnet, is applied along the z direction to magnetize the YIG sphere. The two microwave modes are respectively coupled to a weak probe field (ε_{p_1,p_2}) along the input directions of $a_1^{(\mathrm{in})}$ and $a_2^{(\mathrm{in})}$, which can be regarded as in the transmission of forward and backward directions through a waveguide. The magnon mode in the YIG sphere is diametrically driven by a microwave source with the driving strength ε_d (not shown). In Fig. 1(b), the a_{cw} and a_{ccw} modes are coupled via backscattering with the coupling strength J, and due to the collective magnetic-dipole interaction, the two microwave photons can be coupled to the magnons with the coupling strengths g_1 and g_2 respectively. Without loss of generality, we assume that the coupling strengths g_1, g_2, J are positive numbers and g_1 carries a nontrivial phase ϕ [60]. The nontrivial phase makes the magnon–photon coupling resemble dissipative magnon–photon coupling, which can be caused by the cavity Lenz effect, where the magnons in a magnet induce a RF current in the cavity [25]. Moreover, the

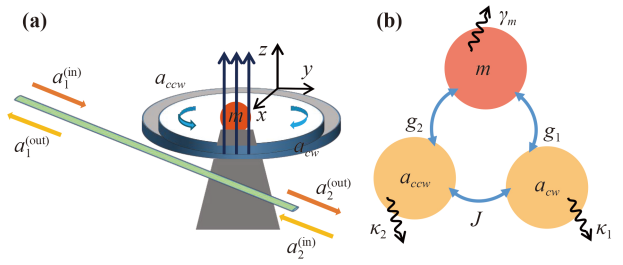

Fig. 1 **(a)** Schematic diagram of a superconducting ring resonator which supports two clockwise (a_{cw}) and counter-clockwise (a_{ccw}) rotating microwave modes, and a YIG sphere which is placed in the middle of the ring resonator. **(b)** Schematic diagram of the linear coupling among the magnon and two microwave modes with the coupling strengths J and $g_{1,2}$ respectively. κ_1, κ_2, γ_m are respectively dissipation rates of two microwave and magnon modes.

phase ϕ can be controlled by changing the YIG location in the cavity. Considering two weak probe fields coupled to the two microwave modes and a strong control field coupled to the magnon mode, the full system can be described by the following Hamiltonian ($\hbar = 1$) [34, 55]:

$$\begin{aligned}\hat{H} =& \omega_0(\hat{a}_{cw}^{\dagger}\hat{a}_{cw} + \hat{a}_{ccw}^{\dagger}\hat{a}_{ccw}) + \omega_m\hat{m}^{\dagger}\hat{m} + K\hat{m}^{\dagger}\hat{m}\hat{m}^{\dagger}\hat{m} \\ &+ (g_1\hat{a}_{cw}^{\dagger}\hat{m}\mathrm{e}^{\mathrm{i}\phi} + g_2\hat{m}^{\dagger}\hat{a}_{ccw} + J\hat{a}_{ccw}^{\dagger}\hat{a}_{cw} + \mathrm{H.C.}) \\ &+ \Big(\sqrt{\kappa_{1,e}/2}\varepsilon_{p_1}\hat{a}_{cw}^{\dagger}\mathrm{e}^{-\mathrm{i}\omega_1 t} + \sqrt{\kappa_{2,e}/2}\varepsilon_{p_2}\hat{a}_{ccw}^{\dagger}\mathrm{e}^{-\mathrm{i}\omega_2 t} \\ &+ \sqrt{\gamma_{m,e}/2}\varepsilon_d\hat{m}^{\dagger}\mathrm{e}^{-\mathrm{i}\omega_d t} + \mathrm{H.C.}\Big),\end{aligned} \tag{1}$$

where ω_0 and ω_m are the resonance frequencies of the two degenerate microwave modes $\hat{a}_i$ ($i = cw, ccw$) and the magnon mode $\hat{m}$ respectively. The frequency of the magnon mode is determined by the static magnetic field H via $\omega_m = \gamma H$, where $\gamma/(2\pi) = 28$ GHz/T is the gyromagnetic ratio. The magnon Kerr nonlinear term $K\hat{m}^{\dagger}\hat{m}\hat{m}^{\dagger}\hat{m}$ in Eq. (1) originates from the magnetocrystalline anisotropy in the YIG, where the positive coefficient $K = \mu_0 K_{an}\gamma/(M^2 V_m)$ with the magnetic permeability of free space μ_0, the first-order anisotropy constant K_{an}, the gyromagnetic ratio γ, the saturation magnetization M, and the volume of the YIG sphere V_m [33]. g_j ($j = 1, 2$) is the linear photon–magnon coupling strength, which can be adjusted by varying the direction of the bias field or the position of the YIG sphere inside the middle of the ring resonator [12]. J is the photon-hopping interaction between two microwave modes. The rest describes the couplings of the driving fields, containing two weak probe fields and a strong control field, to two microwave and magnon modes. The amplitudes of the driving fields are defined as $\varepsilon_{p_j} = \sqrt{P_j/(\hbar\omega_j)}$ and $\varepsilon_d = \sqrt{P_d/(\hbar\omega_d)}$, where the corresponding input power and frequency are $P_{j,d}$ and $\omega_{j,d}$ respectively. $\kappa_{j,e}$ and $\gamma_{m,e}$ are the external coupling rates of the microwave and magnon modes.

Operating on an interaction picture with respect to the free Hamiltonian $\hat{H}_0 = \hbar\omega_d(\hat{a}_{cw}^{\dagger}\hat{a}_{cw} + \hat{a}_{ccw}^{\dagger}\hat{a}_{ccw} + \hat{m}^{\dagger}\hat{m})$, we can obtain

$$\begin{aligned}\dot{\hat{a}}_{cw} =& (-\mathrm{i}\Delta_0 - \kappa_1/2)\hat{a}_{cw} - \mathrm{i}g_1\hat{m}\mathrm{e}^{\mathrm{i}\phi} - \mathrm{i}J\hat{a}_{ccw} \\ &- \mathrm{i}\sqrt{\kappa_{1,e}}\varepsilon_{p_1}\mathrm{e}^{-\mathrm{i}\Omega_1 t} + \sqrt{\kappa_1/2}\hat{a}_{1,\mathrm{in}},\end{aligned} \tag{2}$$

$$\begin{aligned}\dot{\hat{a}}_{ccw} =& (-\mathrm{i}\Delta_0 - \kappa_2/2)\hat{a}_{ccw} - \mathrm{i}g_2\hat{m} - \mathrm{i}J\hat{a}_{cw} \\ &- \mathrm{i}\sqrt{\kappa_{2,e}}\varepsilon_{p_2}\mathrm{e}^{-\mathrm{i}\Omega_2 t} + \sqrt{\kappa_2/2}\hat{a}_{2,\mathrm{in}},\end{aligned} \tag{3}$$

$$\begin{aligned}\dot{\hat{m}} =& (-\mathrm{i}\Delta_m - \gamma_m/2)\hat{m} - \mathrm{i}g_1\hat{a}_{cw}\mathrm{e}^{-\mathrm{i}\phi} - \mathrm{i}g_2\hat{a}_{ccw} \\ &- \mathrm{i}(2K\hat{m}^{\dagger}\hat{m} + K)\hat{m} - \mathrm{i}\sqrt{\gamma_{m,e}}\varepsilon_d + \sqrt{\gamma_m/2}\hat{m}_{\mathrm{in}},\end{aligned} \tag{4}$$

where the rotating-wave approximation (RWA) has been used. The detuning parameters $\Delta_0 = \omega_0 - \omega_d$, $\Delta_m = \omega_m - \omega_d$, and $\Omega_{1,2} = \omega_{p_{1,2}} - \omega_d$. In addition, $\hat{a}_{1,\mathrm{in}}$, $\hat{a}_{2,\mathrm{in}}$ and $\hat{m}_{\mathrm{in}}$ are the input vacuum noises into the microwave photon and magnon modes, respectively. They can be characterized by the following temperature-dependent correlation functions:

$$\langle\hat{a}_{j,\mathrm{in}}(t)\hat{a}_{j,\mathrm{in}}^{\dagger}(t')\rangle = [n_{th}(\omega_0) + 1]\delta(t - t'), \tag{5}$$

$$\langle\hat{a}_{j,\mathrm{in}}^{\dagger}(t)\hat{a}_{j,\mathrm{in}}(t')\rangle = [n_{th}(\omega_0)]\delta(t - t'), \tag{6}$$

$$\langle\hat{m}_{\mathrm{in}}(t)\hat{m}_{\mathrm{in}}^{\dagger}(t')\rangle = [m_{th}(\omega_m) + 1]\delta(t - t'), \tag{7}$$

$$\langle\hat{m}_{\mathrm{in}}^{\dagger}(t)\hat{m}_{\mathrm{in}}(t')\rangle = [m_{th}(\omega_m)]\delta(t - t'), \tag{8}$$

where $n_{th}(\omega_0) = \left[\exp\left(\frac{\hbar\omega_0}{K_B T}\right) - 1\right]^{-1}$, and $m_{th}(\omega_m) = \left[\exp\left(\frac{\hbar\omega_m}{K_B T}\right) - 1\right]^{-1}$ with the Boltzmann constant K_B and the ambient temperature T, are, respectively, the equilibrium means thermal photon and magnon numbers.

In this work, we focus on the mean response of the system, viz. classical equations of motion. Therefore, in the following, the evolution of the system operators can be reduced to their expectation values, viz., $\langle\hat{a}_{cw}\rangle = a_{cw}$, $\langle\hat{a}_{ccw}\rangle = a_{ccw}$, $\langle\hat{m}\rangle = m$. For the sake of convenience, a_{cw} is represented by a_1 and a_{ccw} is represented by a_2. Quantum fluctuation corresponding to the two microwave modes and magnon mode of our system can be neglected because their expectation values are zero. Then, the evolution of the three-mode cavity magnonic system can be described by the Heisenberg-Langevin equations as

$$\dot{a}_1 = (-\mathrm{i}\Delta_0 - \kappa_1/2)a_1 - \mathrm{i}g_1 m\mathrm{e}^{\mathrm{i}\phi} - \mathrm{i}Ja_2 - \mathrm{i}\sqrt{\kappa_{1,e}}\varepsilon_{p_1}\mathrm{e}^{-\mathrm{i}\Omega_1 t}, \tag{9}$$

$$\dot{a}_2 = (-\mathrm{i}\Delta_0 - \kappa_2/2)a_2 - \mathrm{i}g_2 m - \mathrm{i}Ja_1 - \mathrm{i}\sqrt{\kappa_{2,e}}\varepsilon_{p_2}\mathrm{e}^{-\mathrm{i}\Omega_2 t}, \tag{10}$$

$$\dot{m} = (-\mathrm{i}\Delta_m - \gamma_m/2)m - \mathrm{i}g_1 a_1 \mathrm{e}^{-\mathrm{i}\phi} - \mathrm{i}g_2 a_2 - \mathrm{i}(2Km^*m + K)m - \mathrm{i}\sqrt{\gamma_{m,e}}\varepsilon_d. \quad (11)$$

When the control field is much stronger than the probe field, that is $\varepsilon_{p_{1,2}} \ll \varepsilon_d$, we can write each operator for the microwave and magnon modes as a sum of the steady-state and the fluctuation value, i.e., $a_1 = A_{10} + \delta a_1$, $a_2 = A_{20} + \delta a_2$, and $m = M_0 + \delta m$, where the control field provides a steady-state solution of the three-mode cavity magnonic system, and the probe field can be regarded as a perturbation of the steady-state. According to Eqs. (9)–(11), the steady-state solution of the system can be obtained as

$$A_{10} = \frac{-[\mathrm{i}g_1 \mathrm{e}^{\mathrm{i}\phi}(\mathrm{i}\Delta_0 + \kappa_2/2) + Jg_2]M_0}{(\mathrm{i}\Delta_0 + \kappa_1/2)(\mathrm{i}\Delta_0 + \kappa_2/2) + J^2}, \quad (12)$$

$$A_{20} = \frac{-[\mathrm{i}g_2(\mathrm{i}\Delta_0 + \kappa_1/2) + Jg_1 \mathrm{e}^{\mathrm{i}\phi}]M_0}{(\mathrm{i}\Delta_0 + \kappa_1/2)(\mathrm{i}\Delta_0 + \kappa_2/2) + J^2}, \quad (13)$$

$$M_0 = \frac{\sqrt{\gamma_{m,e}}\varepsilon_d}{[(\mathrm{i}\Delta_m' + \gamma_m/2] - \frac{2\mathrm{i}g_1 g_2 J\cos\phi - g_1^2(\mathrm{i}\Delta_0 + \kappa_1/2) - g_2^2(\mathrm{i}\Delta_0 + \kappa_2/2)}{(\mathrm{i}\Delta_0 + \kappa_1/2)(\mathrm{i}\Delta_0 + \kappa_2/2) + J^2}}, \quad (14)$$

where $\Delta_m' = \Delta_m + (2K|M_0|^2 + K)$ is the magnon detuning shifted by the magnon Kerr effect. These equations are coupled to each other and can be solved self-consistently.

Then neglecting the higher nonlinear terms in the magnon Kerr effect in Eqs. (9)–(11), we can obtain a set of linear Heisenberg–Langevin equations for the fluctuation operators:

$$\delta\dot{a}_1 = (-\mathrm{i}\Delta_0 - \kappa_1/2)\delta a_1 - \mathrm{i}g_1 \delta m \mathrm{e}^{\mathrm{i}\phi} - \mathrm{i}J\delta a_2 - \mathrm{i}\sqrt{\kappa_{1,e}}\varepsilon_{p_1}\mathrm{e}^{-\mathrm{i}\Omega_1 t}, \quad (15)$$

$$\delta\dot{a}_2 = (-\mathrm{i}\Delta_0 - \kappa_2/2)\delta a_2 - \mathrm{i}g_2 \delta m - \mathrm{i}J\delta a_1 - \mathrm{i}\sqrt{\kappa_{2,e}}\varepsilon_{p_2}\mathrm{e}^{-\mathrm{i}\Omega_2 t}, \quad (16)$$

$$\delta\dot{m} = (-\mathrm{i}\Delta_m - \gamma_m/2)\delta m - \mathrm{i}g_1 \delta a_1 \mathrm{e}^{-\mathrm{i}\phi} - \mathrm{i}g_2 \delta a_2 - \mathrm{i}[2KM_0^2\delta m^* + (4K \mid M_0 \mid^2 + K)\delta m] - \mathrm{i}\sqrt{\gamma_{m,e}}\varepsilon_d. \quad (17)$$

In order to solve the transmission response of the two microwave modes to the probe field, we make the following ansatz:

$$\delta a_1 = A_{11}^+ \mathrm{e}^{-\mathrm{i}\Omega t} + A_{11}^- \mathrm{e}^{\mathrm{i}\Omega t}, \quad (18)$$

$$\delta a_2 = A_{21}^+ \mathrm{e}^{-\mathrm{i}\Omega t} + A_{21}^- \mathrm{e}^{\mathrm{i}\Omega t}, \quad (19)$$

$$\delta m = M_1^+ \mathrm{e}^{-\mathrm{i}\Omega t} + M_1^- \mathrm{e}^{\mathrm{i}\Omega t}. \quad (20)$$

When $\Omega = \Omega_1$, representing the probe field input from one microwave cavity mode a_1, we mainly focus on the photons of intracavity mode a_2 expressing as A_{21}. On the contrary, when $\Omega = \Omega_2$, representing the probe field input from the other microwave cavity mode a_2, we mainly focus on the photons of intracavity mode a_1 expressing as A_{12}. In what follows, substituting Eqs. (18)–(20) into Eqs. (15)–(17), we can obtain

$$A_{21} = \mathrm{i}g_2(\xi_{m1}^+\xi_{m1}^- - 4K^2M_0^4J^2)\Xi_{14}\sqrt{\eta_1\kappa_1}\varepsilon_{p_1}/\Upsilon_1, \quad (21)$$

$$A_{12} = \mathrm{i}g_1(\xi_{m2}^+\xi_{m2}^- - 4K^2M_0^4J^2)\Xi_{24}\sqrt{\eta_2\kappa_2}\varepsilon_{p_2}/\Upsilon_2, \quad (22)$$

where

$$\Upsilon_1 = \Xi_{12}\Xi_{13} - \Xi_{11}\Xi_{14}, \quad (23)$$

$$\Upsilon_2 = \Xi_{22}\Xi_{23} - \Xi_{21}\Xi_{24}, \quad (24)$$

$$\Xi_{11} = (\mathrm{i}g_2\Delta_1^+\Lambda_2^+ + \mathrm{i}g_1g_2\xi_2^+ + Jg_2\xi_{m1}^+)\xi_{m1}^- - 4K^2M_0^4Jg_2\Lambda^+, \quad (25)$$

$$\Xi_{12} = 2KM_0^2\Delta_2^-\Gamma_1^+\xi_1^- + 2KM_0^2J\zeta_1^+\Lambda_2^-, \quad (26)$$

$$\Xi_{13} = 2KM_0^2\Delta_2^+\Gamma_1^-\xi_1^+ + 2KM_0^2J\zeta_1^-\Lambda_2^+, \quad (27)$$

$$\Xi_{14} = (\mathrm{i}g_2\Delta_1^-\Lambda_2^- + \mathrm{i}g_1g_2\xi_2^- + Jg_2\xi_{m1}^-)\xi_{m1}^+ - 4K^2M_0^4Jg_2\Lambda^-, \quad (28)$$

$$\Xi_{21} = (\mathrm{i}g_1\Delta_2^+\mathrm{e}^{\mathrm{i}\phi}\Lambda_1^+ + \mathrm{i}g_1g_2\xi_1^+ + Jg_1\xi_{m2}^+\mathrm{e}^{\mathrm{i}\phi})\xi_{m2}^- - 4K^2M_0^4Jg_1\mathrm{e}^{\mathrm{i}\phi}\Lambda^+, \quad (29)$$

$$\Xi_{22} = 2KM_0^2\Delta_1^-\Gamma_2^+\xi_2^- + 2KM_0^2J\zeta_2^+\Lambda_1^-, \quad (30)$$

$$\Xi_{23} = 2KM_0^2\Delta_1^+\Gamma_2^-\xi_2^+ + 2KM_0^2J\zeta_2^-\Lambda_1^+, \quad (31)$$

$$\Xi_{24} = (\mathrm{i}g_1\Delta_2^-\mathrm{e}^{\mathrm{i}\phi}\Lambda_1^- + \mathrm{i}g_1g_2\xi_1^- + Jg_1\xi_{m2}^-\mathrm{e}^{\mathrm{i}\phi})\xi_{m2}^+ - 4K^2M_0^4Jg_1\Lambda^-, \quad (32)$$

and $\Delta_1^\pm = -\mathrm{i}(\Delta_0 \mp \Omega) - \kappa_1/2$, $\Delta_2^\pm = -\mathrm{i}(\Delta_0 \mp \Omega) - \kappa_2/2$, $\Delta_m^\pm = -\mathrm{i}(\Delta_m \mp \Omega + 4K \mid M_0 \mid^2 + K) - \gamma_m/2$, $\xi_1^\pm = g_2\Delta_1^\pm\mathrm{e}^{\mathrm{i}\phi} + \mathrm{i}Jg_1$, $\xi_2^\pm = g_1\Delta_2^\pm + \mathrm{i}Jg_2\mathrm{e}^{\mathrm{i}\phi}$, $\xi_{m1}^\pm = \mathrm{i}J\Delta_m^\pm - g_1g_2\mathrm{e}^{-\mathrm{i}\phi}$, $\xi_{m2}^\pm = \mathrm{i}J\Delta_m^\pm - g_1g_2\mathrm{e}^{\mathrm{i}\phi}$, $\Lambda_1^\pm = \Delta_1^\pm\Delta_m^\pm + g_1^2$, $\Lambda_2^\pm = \Delta_2^\pm\Delta_m^\pm + g_2^2$, $\Lambda^\pm = \Delta_1^\pm\Delta_2^\pm + J^2$, $\zeta_1^\pm = Jg_1\mathrm{e}^{\mathrm{i}\phi} - \mathrm{i}g_2\Delta_1^\pm$, $\zeta_2^\pm = Jg_2 - \mathrm{i}g_1\Delta_2^\pm\mathrm{e}^{\mathrm{i}\phi}$, $\Gamma_1^\pm = g_2\Delta_1^\pm + \mathrm{i}Jg_1\mathrm{e}^{\mathrm{i}\phi}$, $\Gamma_2^\pm = g_1\Delta_2^\pm\mathrm{e}^{\mathrm{i}\phi} + \mathrm{i}Jg_2$. According to the standard input-output relation [61, 62], the output fields $a_2^{(\mathrm{out})}$ and $a_1^{(\mathrm{out})}$ can be written as follows:

$$a_2^{(\mathrm{out})} = -\sqrt{\kappa_{2,e}}A_{21}, \quad (33)$$

$$a_1^{(\mathrm{out})} = -\sqrt{\kappa_{1,e}}A_{12}. \quad (34)$$

Then we define T_{21} and T_{12} as the transmission coefficients for the probe field input from $a_1^{(\mathrm{in})}$ and $a_2^{(\mathrm{in})}$ directions, with

$$T_{21} \equiv |\frac{a_2^{(\mathrm{out})}}{\varepsilon_{p_1}}|, \qquad T_{12} \equiv |\frac{a_1^{(\mathrm{out})}}{\varepsilon_{p_2}}|. \tag{35}$$

It can be seen that it is very difficult and tedious to give an analytical and simplified solution to the two output fields. To verify our theory and show the nonreciprocal microwave transmission in this cavity magnonic system under the joint mechanism of phase modulation and magnon Kerr nonlinearity effect, a more convenient practice is to use numerical calculations based on existing expressions.

In order to intuitively observe the differences between the output fields $|a_2^{(\mathrm{out})}|^2$ and $|a_1^{(\mathrm{out})}|^2$, we define a dimensionless quantity I to describe the efficiency of the nonreciprocal transmission of the probe field, regarded as the isolation ratio:

$$I = 10\left|\log_{10}\frac{|a_2^{(\mathrm{out})}|^2}{|a_1^{(\mathrm{out})}|^2}\right|, \tag{36}$$

with the unit of I being dB. If $I=0$, that is $|a_2^{(\mathrm{out})}|^2/|a_1^{(\mathrm{out})}|^2 = 1$, which represents one case of reciprocal transmission. When the value of I is nonzero, it presents another case of nonreciprocal transmission, and the greater the value of I, the higher degree of the nonreciprocal transmission of the probe field.

To study the nonreciprocal transmission of the probe field under the joint mechanism of phase modulation and magnon Kerr nonlinearity effect, we plot Fig. 2(a), which shows the calculation results of isolation ratio I vary with the total phase difference ϕ and the pump power P_d of the control field. We use $\omega_m/(2\pi) = 10.1$ GHz, $\kappa_1/(2\pi) = 3.8$ MHz, $\gamma_m/(2\pi) = 17.5$ MHz, $J/(2\pi) = 20$ MHz, $g_1/(2\pi) = 41$ MHz, $K/\kappa_1 = 10^{-10}$. According to $K = \mu_0 K_{an}\gamma/(M^2 V_m)$, we know that the Kerr coefficient is inversely proportional to V_m, i.e., $K \propto V_m^{-1}$. Once the diameter size of the YIG sphere can be reduced to about 10 microns, the value of K can be increased by three orders of magnitude from the previous several hundred nHz [33]. Until now, nanoscale magnetic particles [6, 63] are already common, and so we think the micron-sized YIG sphere is very possible in experiment. It can be observed that the bright regions are symmetrically distributed about the center of phase $\phi = \pi$. On the one hand, when $\phi = 0$ or 2π, the areas we see remain dark with the increase of the pump power, which indicates that in the absence of phase effect, the current magnon Kerr nonlinearity effect is too weak to cause nonreciprocity. On the other hand, when $P_d = 0$ mW, the value of I is always several dB as the phase changes. These suggest that based on the existing parameters, it is difficult to achieve strong nonreciprocal transmission

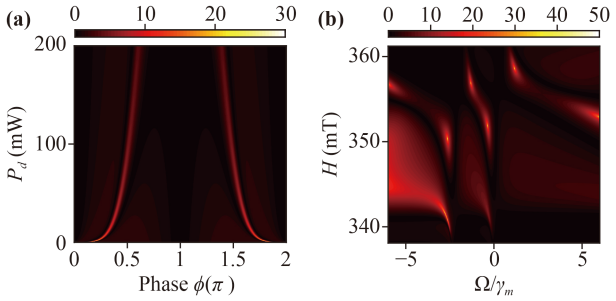

Fig. 2 **(a)** The calculation results of the isolation ratio I (dB) vary with the phase ϕ and the power P_d of the control field, where $\Delta_m = \Omega_{1,2} = \gamma_m$. **(b)** The calculation results of the isolation ratio I (dB) vary with the frequency detuning Ω and the external magnetic field H, where $\phi = \pi/2$, $P_d = 100$ mW. The other parameters are $\omega_m/(2\pi) = 10.1$ GHz, $\kappa_1/(2\pi) = 3.8$ MHz, $\kappa_2 = \kappa_1$, $\gamma_m/(2\pi) = 17.5$ MHz, $J/(2\pi) = 20$ MHz, $g_1/(2\pi) = 41$ MHz, $g_2 = g_1$, $K/\kappa_1 = 10^{-10}$, $\kappa_{1,e} = 0.5\kappa_1$, $\kappa_{2,e} = 0.5\kappa_2$, $\gamma_{m,e} = 0.5\gamma_m$, $\Delta_0 = \gamma_m$, which are based on the latest experimental parameters [21, 33].

only under the single mechanism of phase modulation or magnon Kerr nonlinearity effect. Moreover, we find that the value of I does not increase monotonically with the power enhanced, which is attributed to the destructive coherence between the phase modulation and the magnon Kerr nonlinearity effect. Based on the available experimental parameters, the power range required for obtaining large isolation rates is mainly concentrated in the range less than 100 mW. In addition, to simplify, we will present a discussion of the nonreciprocal transmission of the probe field in the range of $\phi \in (0, \pi/2)$ in what follows.

The calculation results of isolation ratio I plotted as a function of the frequency detuning Ω and the external magnetic field H are shown in Fig. 2(b), which gives us a clear perspective for the tunability of the probe field and the magnetic field. Figure 2(b) shows an obvious level repulsion of the hybridized three modes and several separated gaps, which are determined by the coupling strength among them. It can be observed that the frequency of the magnon corresponding to the operating range of the H is compared to the Ω, with greater adjustable range (about 4 times) to obtain the strong nonreciprocal transmission. These results confirm that such a microwave nonreciprocity system with a large isolation ratio could be obtained from a ring resonator cavity within a small YIG sphere, and its essential factor originates from the joint action of the phase modulation and the magnon Kerr nonlinearity effect.

3 The features of nonreciprocal microwave transmission

Different from the previous research of nonreciprocal transmission based on general phase [48] or magnon

Kerr nonlinearity effect [57], in this work, we will in detail discuss the joint effects of phase modulation and magnon Kerr nonlinearity on the nonreciprocal transmission of the probe field. According to the Eqs. (35) and (36), the curves plotted for the transmission coefficients and the isolation ratios of the probe field are shown in Fig. 3, which reveals the differences of the microwave transmission along forward and backward directions under various pump powers of the control field. Figure 3(a) exhibits the transmission coefficients at a linear response system when $P_{\rm d} = 0$ mW. It can be found that two transmission coefficients T_{21} (blue solid curve) and T_{12} (red dashed curve) are symmetrically distributed with respect to $\Omega = \gamma_m$ due to $\Delta_0 = \Delta_m = \gamma_m$, and the three prominent peaks are induced by the hybridization between microwave photons and magnons. With the increase of the power $P_{\rm d}$ in Fig. 3(b), both the locations of the peaks of T_{21} and T_{12} have changed greatly, and the amplitude intensity of the transmission coefficients is also enhanced, which indicates the magnon Kerr nonlinearity effect has played a role.

According to the description of Figs. 3(a) and (b), we find that when $\phi = \pi/2$ in Fig. 3, relatively high power is needed to realize the nonreciprocal microwave transmission. In order not to increase the power, we attempt to transform other variables, such as the magnon–photon coupling strength, which can be engineered by changing the microwave mode volume and frequency, engineering the field overlap, and utilizing materials with different spin densities, to achieve the nonreciprocal transmission

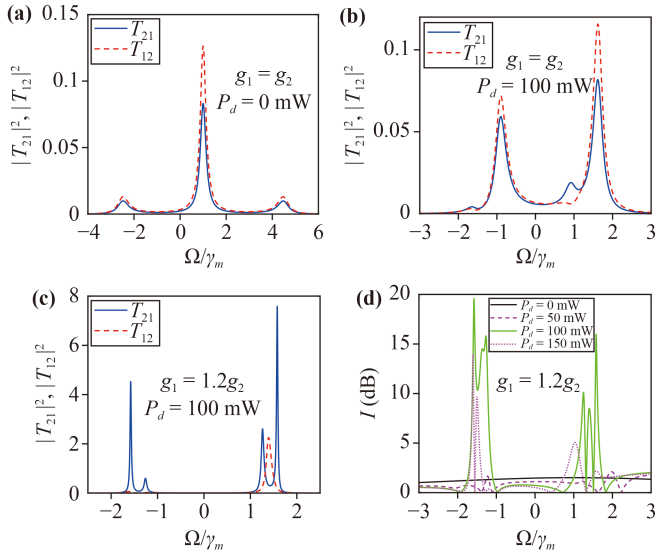

Fig. 3 **(a–c)** Transmission coefficients T_{21} (blue solid curve) and T_{12} (red dashed curve) are plotted as functions of the frequency detuning Ω for different g_2 and the powers P_d of the control field. **(d)** The calculation results of the isolation ratio $\boldsymbol{I}$ vary with the frequency detuning Ω under different powers P_d of the control field. We use $\phi = \pi/2$, and the other parameters are the same as in Fig. 2.

of the probe field. During experimental measurements, the coupling strength can be tuned dynamically by changing the position between the YIG sphere and the circuit to effectively tune the field overlap factor, adding an additional ground plate to modify the microwave field distribution, and tuning the temperature [55]. Therefore, we draw Fig. 3(c) with $g_2 = 1.2g_1$. It can be observed that especially for T_{21}, there are two significant pattern splits for the original two peaks, then becoming four evident peak points. Moreover, the spacing between two adjacent peaks becomes narrower and the intensity of the T_{21} and T_{12} gets amplified. This explains that under this condition, the magnon Kerr nonlinearity effect makes the system essentially change, and the change is positive, which makes the obtained nonreciprocal effect stronger. In particular, when Ω is in the range of about $-2\gamma_m$ to $-\gamma_m$ or γ_m to $2\gamma_m$, where the range of the probe field corresponding to operating bandwidth can reach dozens MHz, we can obtain a large isolation ratio, which benefits from the constructive coherence of the phase modulation and the magnon Kerr nonlinearity effect. To understand the differences between the transmission coefficients T_{21} and T_{12} more intuitively, the calculation results of I are shown in Fig. 3(d) for different powers. When the power is set to 100 mW, the maximum isolation rate reaches 19.6 dB. However, when the power increases to 150 mW, the isolation rate of the maximum value decreases to 16 dB, which indicates the effect of the joint mechanism of phase modulation and magnon Kerr nonlinearity effect is no longer increased, but suppressed when the control field power exceeds a certain threshold.

In order to understand the influence of different phases on the nonreciprocal transmission of the probe field, we give the numerical simulations of the transmission coefficient in Fig. 4. Here we adjust the magnitude of the relative phase ϕ to $\pi/4$, and find that $\pi/4$ is the optimal magnitude of the phase for the nonreciprocal transmission. Compared to Fig. 3(a), only the positions of the peaks have changed in Fig. 4(a), where the nonreciprocal transmission of the probe field is less obvious. Once we enhance the power to 4 mW in Fig. 4(b), two curves of the transmission coefficients T_{21} and T_{12}, have changed substantially in comparison with Fig. 4(a). The magnon Kerr nonlinearity effect starts to play a role and leads to three-mode split, where we can observe four peak points.

Moreover, the range of the frequency detuning Ω for obtaining the nonreciprocal transmission also gets increased, that is the adjustable isolation bandwidth about 68 MHz from $-\gamma_m$ to γ_m. As the power increases to 10 mW in Fig. 4(c), it is unexpected to find that not only the value of T_{21} and T_{12} is decreased, but also the split patterns tend to merge instead. Finally, when we consider $P_d = 100$ mW to continue to enhance the magnon Kerr nonlinearity effect in Fig. 4(d), the nonreciprocity effect also has a tendency to decline on the

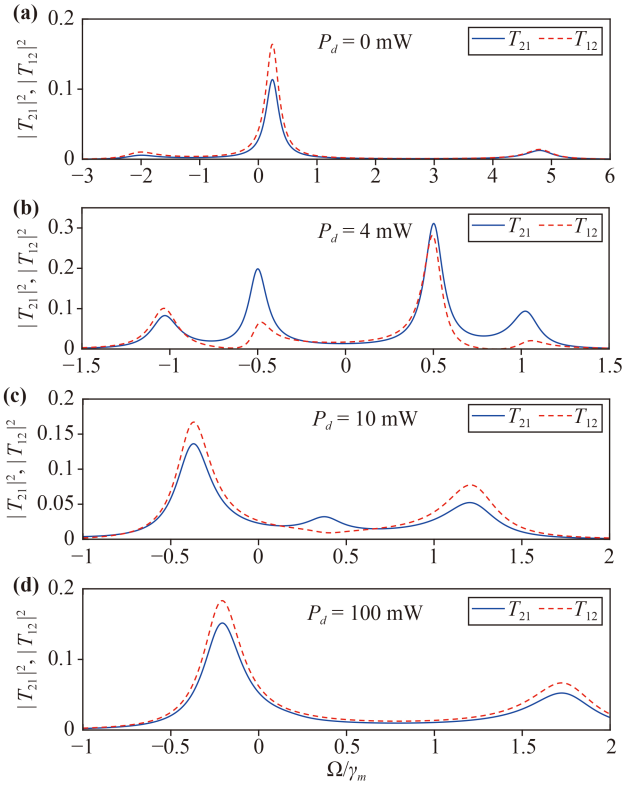

Fig. 4 Transmission coefficients T_{21} (blue solid curve) and T_{12} (red dashed curve) are plotted as functions of the frequency detuning Ω under different powers P_d of the control field. From **(a)** to **(d)**, P_d is 0 mW, 4 mW, 10 mW, 100 mW respectively. We use $\phi = \pi/4$, and the other parameters are the same as in Fig. 2.

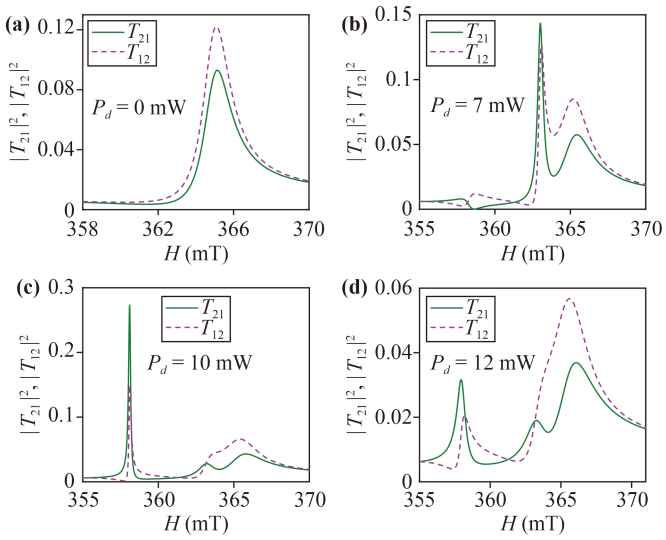

Fig. 5 Transmission coefficients T_{21} (greed solid curve) and T_{12} (purple dashed curve) are plotted as functions of the external magnetic field H under different powers P_d of the control field. From **(a)** to **(d)**, P_d is 0 mW, 7 mW, 10 mW, 12 mW respectively. We use $\phi = \pi/4$, and the other parameters are the same as in Fig. 2.

contrary. This reveals that in some circumstances, the quantum interference induced by the phase modulation between multiple channels and the magnon Kerr nonlinearity effect can be mutually inhibited, which is not conducive to the generation of nonreciprocal transmission.

According to the above exhibition of nonreciprocal microwave transmission regulated by the frequency detuning Ω shown in Figs. 3 and 4, it is found that when the nonreciprocal transmission can be realized, the adjustable frequency range of the probe field is not very large. Therefore, for the sake of expanding the operability on manipulating the nonreciprocal transmission, we try to change another variable, i.e., the external magnetic field, which is generated by a superconducting magnet to magnetize the YIG sphere and can be varied over a wide range (from 0 to 1 T). Figure 5 shows the transmission coefficients T_{21} (greed solid curve) and T_{12} (purple dashed curve) as functions of the external magnetic field H for different powers P_{d} of the control field.

In Fig. 5(a), one can see that the curve changes of both T_{21} and T_{12} are relatively smooth in a linear response system with $P_d = 0$ mW. When we consider applying an external drive to the magnon mode in Figs. 5(b) and (c), peaks and troughs of the tips begin to appear, which explains that the magnon Kerr nonlinearity effect plays a role in the nonreciprocal transmission of the probe field. In addition, the difference value between T_{21} and T_{12} is gradually pulling apart, that is, the effect of the nonreciprocal transmission is gradually increasing. As the power continues to increase, we can find that the operating range of the magnetic field for observing the nonreciprocal microwave transmission is also enlarged, but the amplitude intensities of the transmission coefficients decrease instead, as shown in Fig. 5(d). Therefore, the use of magnetic field can indeed enlarge the adjustable range of nonreciprocal transmission and enhance the practical application value, but the isolation ratio of nonreciprocal transmission has not been significantly improved.

In order to effectively raise the isolation ratio I of the nonreciprocal microwave transmission, we show the value of I as functions of the external magnetic field H for different powers P_d in Fig. 6, with two different g_2. As a contrast, we plot Fig. 6(a), where $g_1 = g_2$, and one can observe that as the magnetic field changes, the obtained value of I is almost no more than 6 dB. However, when $g_1 = 1.3g_2$, which induces the optimal possible results in Fig. 6(b), there exists an extremely large magnetic tunable region that causes the value of I to exceed 10 dB, which presents a great difference on the transmission of the probe field between the forward and backward incidences. Especially when the power is equal to 12 or 16 mW, not only the value of I is significantly improved, but also it enables us to obtain a high isolation rate (>20 dB) that can be manipulated by the magnetic

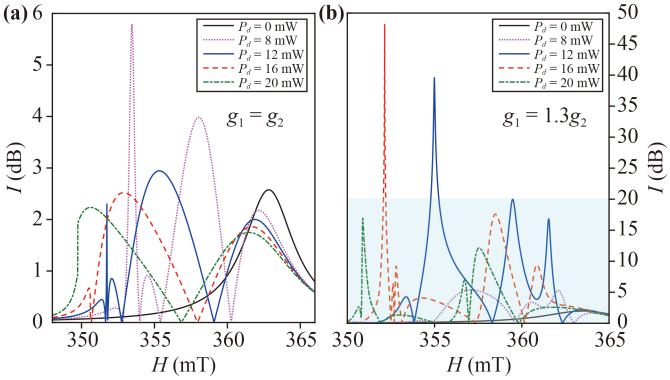

Fig. 6 The isolation ratios I of the nonreciprocal microwave transmission are plotted as functions of the external magnetic field H under different powers P_d of the control field and g_2. We use $\phi = \pi/4$, and the other parameters are the same as in Fig. 2.

field in a large adjustable range, and its corresponding to the operating bandwidths can reach thousands MHz. This indicates that two different cavity-magnon couplings are very beneficial to the realization of the strong nonreciprocal microwave transmission. In addition, as the power increases gradually [seeing the green dotted line], the value of the corresponding isolation ratio is decreasing on the whole, which may be due to the destructive coherence between phase modulation and magnon Kerr nonlinearity effect. Finally, we can conclude that when two microwave modes are coupled to the magnon mode via a different coupling strength, the strong nonreciprocal transmission can be obtained even at low power.

4 Conclusions

In summary, the nonreciprocal microwave transmission under the joint mechanism of phase modulation and magnon Kerr nonlinear effect has been studied in a three-mode cavity magnonics system. In order to describe the characteristics of nonreciprocal transmission under the above joint mechanism, we employed the quantum Langevin equation under rotating wave approximation by using the perturbation method. By taking advantage of the magnetic field with a intrinsically good flexibility, we have exhibited a variable nonreciprocal transmission at different phases and powers of the control field. In contrast to using the phase difference or magnon Kerr nonlinearity effect, we find that the modulation of the twofold mechanism makes the nonreciprocal transmission occur even at low power and its effect can be further enhanced under certain conditions. In addition, when two microwave modes are coupled to the magnon mode via a different coupling strength, it is found that the isolation rate can get drastically enhanced within a certain range of power and we can obtain the strong nonreciprocal transmission with a large tunable range of the magnetic field, which is the result of the constructive coherence of quantum interference induced by the phase difference and magnon Kerr nonlinearity effect. These exotic features of the three-cavity magnonics system extremely widen new perspectives for exploring the nonreciprocity, and it has great potential applications in magnetically controlled isolators, optical diodes and so on.

Acknowledgements The work was supported by the National Natural Science Foundation of China (Grant Nos. 12105092 and 12022507) and Program for Innovative Teams of Outstanding Young and Middle-aged Researchers in the Higher Education Institution of Hubei Province (No. T2020014).

References

1. H. Walther, B. T. H. Varcoe, B. G. Englert, and T. Becker, Cavity quantum electrodynamics, *Rep. Prog. Phys.* 69(5), 1325 (2006)
2. Q. P. Su, Y. Zhang, L. Bin, and C. P. Yang, Efficient scheme for realizing a multiplex-controlled phase gate with photonic qubits in circuit quantum electrodynamics, *Front. Phys.* 17(5), 53505 (2022)
3. D. D. Stancil and A. Prabhakar, Spin Waves, Springer, New York, 2009
4. Ö. O. Soykal and M. E. Flatté, Strong field interactions between a nanomagnet and a photonic cavity, *Phys. Rev. Lett.* 104(7), 077202 (2010)
5. B. Zare Rameshti, Y. Cao, and G. E. W. Bauer, Magnetic spheres in microwave cavities, *Phys. Rev. B* 91(21), 214430 (2015)
6. Y. Tabuchi, S. Ishino, A. Noguchi, T. Ishikawa, R. Yamazaki, K. Usami, and Y. Nakamura, Coherent coupling between a ferromagnetic magnon and a superconducting qubit, *Science* 349(6246), 405 (2015)
7. J. Shim, S. J. Kim, S. K. Kim, and K. J. Lee, Enhanced magnon–photon coupling at the angular momentum compensation point of ferrimagnets, *Phys. Rev. Lett.* 125(2), 027205 (2020)
8. K. Wang, Y. P. Gao, R. Z. Jiao, and C. Wang, Recent progress on optomagnetic coupling and optical manipulation based on cavity-optomagnonics, *Front. Phys.* 17(4), 42201 (2022)
9. H. J. Kimble, The quantum internet, *Nature* 453(7198), 1023 (2008)
10. M. Aspelmeyer, T. J. Kippenberg, and F. Marquardt, Cavity optomechanics, *Rev. Mod. Phys.* 86(4), 1391 (2014)
11. J. W. Zhou, P. F. Wang, F. Z. Shi, P. Huang, X. Kong, X. K. Xu, Q. Zhang, Z. X. Wang, X. Rong, and J. F. Du, Quantum information processing and metrology with color centers in diamonds, *Front. Phys.* 9(5), 587 (2014)
12. X. Zhang, C. L. Zou, L. Jiang, and H. X. Tang, Strongly coupled magnons and cavity microwave photons, *Phys. Rev. Lett.* 113(15), 156401 (2014)

13. M. Goryachev, W. G. Farr, D. L. Creedon, Y. Fan, M. Kostylev, and M. E. Tobar, High-cooperativity cavity QED with magnons at microwave frequencies, *Phys. Rev. Appl.* 2(5), 054002 (2014)
14. D. Zhang, X.-M. Wang, T.-F. Li, X.-Q. Luo, W. Wu, F. Nori, and J. Q. You, Cavity quantum electrodynamics with ferromagnetic magnons in a small yttrium-iron-garnet sphere, *npj Quantum Inf.* 1, 15014 (2015)
15. B. Yao, Y. Gui, J. Rao, S. Kaur, X. Chen, W. Lu, Y. Xiao, H. Guo, K. P. Marzlin, and C. M. Hu, Cooperative polariton dynamics in feedback-coupled cavities, *Nat. Commun.* 8(1), 1437 (2017)
16. Y. Tabuchi, S. Ishino, T. Ishikawa, R. Yamazaki, K. Usami, and Y. Nakamura, Hybridizing ferromagnetic magnons and microwave photons in the quantum limit, *Phys. Rev. Lett.* 113(8), 083603 (2014)
17. N. Kostylev, M. Goryachev, and M. E. Tobar, Superstrong coupling of a microwave cavity to yttrium iron garnet magnons, *Appl. Phys. Lett.* 108(6), 062402 (2016)
18. J. Bourhill, N. Kostylev, M. Goryachev, D. Creedon, and M. Tobar, Ultrahigh cooperativity interactions between magnons and resonant photons in a YIG sphere, *Phys. Rev. B* 93(14), 144420 (2016)
19. G. Flower, M. Goryachev, J. Bourhill, and M. E. Tobar, Experimental implementations of cavity-magnon systems: From ultra strong coupling to applications in precision measurement, *New J. Phys.* 21(9), 095004 (2019)
20. L. Bai, M. Harder, Y. P. Chen, X. Fan, J. Q. Xiao, and C. M. Hu, Spin pumping in electrodynamically coupled magnon–photon systems, *Phys. Rev. Lett.* 114(22), 227201 (2015)
21. Y. P. Wang, G. Q. Zhang, D. Zhang, T. F. Li, C. M. Hu, and J. Q. You, Bistability of cavity magnon polaritons, *Phys. Rev. Lett.* 120(5), 057202 (2018)
22. X. F. Zhang, C. L. Zou, N. Zhu, F. Marquardt, L. Jiang, and H. X. Tang, Magnon dark modes and gradient memory, *Nat. Commun.* 6(1), 8914 (2015)
23. R. C. Shen, Y. P. Wang, J. Li, S. Y. Zhu, G. S. Agarwal, and J. Q. You, Long-time memory and ternary logic gate using a multistable cavity magnonic system, *Phys. Rev. Lett.* 127(18), 183202 (2021)
24. Y. P. Wang and C. M. Hu, Dissipative couplings in cavity magnonics, *J. Appl. Phys.* 127(13), 130901 (2020)
25. M. Harder, Y. Yang, B. M. Yao, C. H. Yu, J. W. Rao, Y. S. Gui, R. L. Stamps, and C. M. Hu, Level attraction due to dissipative magnon–photon coupling, *Phys. Rev. Lett.* 121(13), 137203 (2018)
26. J. W. Rao, C. H. Yu, Y. T. Zhao, Y. S. Gui, X. Fan, D. Xue, and C. M. Hu, Level attraction and level repulsion of magnon coupled with a cavity anti-resonance, *New J. Phys.* 21(6), 065001 (2019)
27. Y. Cao, P. Yan, H. Huebl, S. T. B. Goennenwein, and G. E. W. Bauer, Exchange magnon-polaritons in microwave cavities, *Phys. Rev. B* 91(9), 094423 (2015)
28. L. Bai, M. Harder, P. Hyde, Z. Zhang, C. M. Hu, Y. P. Chen, and J. Q. Xiao, Cavity mediated manipulation of distant spin currents using a cavity-magnon-polariton, *Phys. Rev. Lett.* 118(21), 217201 (2017)
29. D. Zhang, X. Q. Luo, Y. P. Wang, T. F. Li, and J. Q. You, Observation of the exceptional point in cavity magnon-polaritons, *Nat. Commun.* 8(1), 1368 (2017)
30. G. Q. Zhang and J. Q. You, Higher-order exceptional point in a cavity magnonics system, *Phys. Rev. B* 99(5), 054404 (2019)
31. R. Huang, Ş. K. Özdemir, J. Q. Liao, F. Minganti, L. M. Kuang, F. Nori, and H. Jing, Exceptional photon blockade: engineering photon blockade with chiral exceptional points, *Laser Photonics Rev.* 16(7), 2100430 (2022)
32. Z. X. Yang, L. Wang, Y. M. Liu, D. Y. Wang, C. H. Bai, S. Zhang, and H. F. Wang, Ground state cooling of magnomechanical resonator in *PT*-symmetric cavity magnomechanical system at room temperature, *Front. Phys.* 15(5), 52504 (2020)
33. G. Q. Zhang, Y. P. Wang, and J. Q. You, Theory of the magnon Kerr effect in cavity magnonics, *Sci. China Phys. Mech. Astron.* 62(8), 987511 (2019)
34. Y. P. Wang, G. Q. Zhang, D. Zhang, X. Q. Luo, W. Xiong, S. P. Wang, T. F. Li, C. M. Hu, and J. Q. You, Magnon Kerr effect in a strongly coupled cavity-magnon system, *Phys. Rev. B* 94(22), 224410 (2016)
35. Z. B. Yang, H. Jin, J. W. Jin, J. Y. Liu, H. Y. Liu, and R. C. Yang, Bistability of squeezing and entanglement in cavity magnonics, *Phys. Rev. A* 3, 023126 (2021)
36. Z. Haghshenasfarda and M. G. Cottam, Sub-Poissonian statistics and squeezing of magnons due to the Kerr effect in a hybrid coupled cavity-magnon system, *J. Appl. Phys.* 128(3), 033901 (2020)
37. Z. X. Liu, B. Wang, H. Xiong, and Y. Wu, Magnon-induced high-order sideband generation, *Opt. Lett.* 43(15), 3698 (2018)
38. Y. L. Liu, L. Ling, T. Shui, N. Ji, S. P. Liu, and W. X. Yang, Two-color second-order sideband generation via magnon Kerr nonlinearity in a cavity magnonical system, *J. Opt. Soc. Am. B* 39, 1042 (2022)
39. Z. X. Liu, C. You, B. Wang, H. Xiong, and Y. Wu, Phase-mediated magnon chaos-order transition in cavity optomagnonics, *Opt. Lett.* 44(3), 507 (2019)
40. Y. P. Wang, J. W. Rao, Y. Yang, P. C. Xu, Y. S. Gui, B. M. Yao, J. Q. You, and C. M. Hu, Nonreciprocity and unidirectional invisibility in cavity magnonics, *Phys. Rev. Lett.* 123(12), 127202 (2019)
41. Z. B. Yang, J. S. Liu, A. D. Zhu, H. Y. Liu, and R. C. Yang, Nonreciprocal transmission and nonreciprocal entanglement in a spinning microwave magnomechanical system, *Ann. Phys.* 532(9), 2000196 (2020)
42. X. B. Yan, H. L. Lu, F. Gao, and L. Yang, Perfect optical nonreciprocity in a double-cavity optomechanical system, *Front. Phys.* 14(5), 52601 (2019)
43. S. Y. Hua, J. M. Wen, X. S. Jiang, Q. Hua, L. Jiang, and M. Xiao, Demonstration of a chip-based optical isolator with parametric amplification, *Nat. Commun.* 7(1), 13657 (2016)
44. Y. Tokura, M. Kawasaki, and N. Nagaosa, Emergent functions of quantum materials, *Nat. Phys.* 13(11), 1056 (2017)
45. P. Doyeux, S. A. H. Gangaraj, G. W. Hanson, and M. Antezza, Giant interatomic energy-transport amplification with nonreciprocal photonic topological insulators, *Phys. Rev. Lett.* 119(17), 173901 (2017)
46. F. D. M. Haldane and S. Raghu, Possible realization of directional optical wave-guides in photonic crystals with

broken time-reversal symmetry, *Phys. Rev. Lett.* 100(1), 013904 (2008)
47. Y. Hadad and B. Z. Steinberg, Magnetized spiral chains of plasmonic ellipsoids for one-way optical waveguides, *Phys. Rev. Lett.* 105(23), 233904 (2010)
48. X. X. Guo, Y. M. Ding, Y. Duan, and X. J. Ni, Nonreciprocal metasurface with space-time phase modulation, *Light Sci. Appl.* 8(1), 123 (2019)
49. M. S. Kang, A. Butsch, and P. S. J. Russell, Reconfigurable light-driven opto-acoustic isolators in photonic crystal fibre, *Nat. Photonics* 5(9), 549 (2011)
50. Y. Shi, Z. F. Yu, and S. H. Fan, Limitations of nonlinear optical isolators due to dynamic reciprocity, *Nat. Photonics* 9(6), 388 (2015)
51. A. B. Khanikaev and A. Alù, Nonlinear dynamic reciprocity, *Nat. Photonics* 9(6), 359 (2015)
52. T. Shui, W. X. Yang, M. T. Cheng, and R. K. Lee, Optical nonreciprocity and nonreciprocal photonic devices with directional four-wave mixing effect, *Opt. Express* 30(4), 6284 (2022)
53. X. Y. Huang, C. C. Lu, C. Liang, H. G. Tao, and Y. C. Liu, Loss-induced nonreciprocity, *Light: Sci. Appl.* 10(1), 30 (2021)
54. Y. T. Zhao, J. W. Rao, Y. S. Gui, Y. P. Wang, and C. M. Hu, Broadband nonreciprocity realized by locally controlling the magnon's radiation, *Phys. Rev. Appl.* 14(1), 014035 (2020)
55. N. Zhu, X. Han, C. L. Zou, M. R. Xu, and H. X. Tang, Magnon–photon strong coupling for tunable microwave circulators, *Phys. Rev. A* 101(4), 043842 (2020)
56. X. F. Zhang, A. Galda, X. Han, D. F. Jin, and V. M. Vinokur, Broadband nonreciprocity enabled by strong coupling of magnons and microwave photons, *Phys. Rev. Appl.* 13(4), 044039 (2020)
57. C. Kong, H. Xiong, and Y. Wu, Magnon-induced nonreciprocity based on the magnon Kerr effect, *Phys. Rev. Appl.* 12(3), 034001 (2019)
58. C. Kong, X. M. Bao, J. B. Liu, and H. Xiong, Magnon-mediated nonreciprocal microwave transmission based on quantum interference, *Opt. Lett.* 29, 16 (2021)
59. S. Manipatruni, J. T. Robinson, and M. Lipson, Optical nonreciprocity in optomechanical structures, *Phys. Rev. Lett.* 102(21), 213903 (2009)
60. A. Metelmann and A. A. Clerk, Nonreciprocal photon transmission and amplification via reservoir engineering, *Phys. Rev. X* 5(2), 021025 (2015)
61. C. Ciuti and I. Carusotto, Input–output theory of cavities in the ultrastrong coupling regime: The case of time-independent cavity parameters, *Phys. Rev. A* 74(3), 033811 (2006)
62. C. W. Gardiner and P. Zoller, Quantum Noise, Springer, 2004
63. J. T. Hou and L. Q. Liu, Strong coupling between microwave photons and nanomagnet magnons, *Phys. Rev. Lett.* 123(10), 107702 (2019)